

# The pseudo-symmetric optimization of the National Compact Stellarator Experiment

M. Yu. Isaev and M. I. Mikhailov

*Nuclear Fusion Institute, Russian Research Centre "Kurchatov Institute," 123182 Moscow, Russia*

D. A. Monticello and H. E. Mynick

*Princeton Plasma Physics Laboratory, Princeton, New Jersey*

A. A. Subbotin

*Nuclear Fusion Institute, Russian Research Centre "Kurchatov Institute," 123182 Moscow, Russia*

L. P. Ku and A. H. Reiman

*Princeton Plasma Physics Laboratory, Princeton, New Jersey*

(Received 19 January 1999; accepted 19 April 1999)

A new experiment, the National Compact Stellarator Experiment (NCSX) [Monticello *et al.* "Physics Consideration for the Design of NCSX," *Proceedings of 25th EPS Conference on Controlled Fusion and Plasma Physics, Prague, 1998* (European Physical Society, Petit-Lancy), paper 1.187], hopes to overcome the deleterious ripple transport usually associated with stellarators by creating a quasi-axisymmetric configuration. A quasi-axisymmetric configuration is one in which the Fourier spectrum of the magnetic field strength in so-called Boozer coordinates is dominated by the toroidal angle averaged ( $n=0$ ) components. In this article the concept of pseudosymmetry is used to improve ripple transport in a four-period variant of NCSX. By definition, pseudosymmetric magnetic configurations have no locally trapped particles. To obtain a pseudosymmetric configuration, different target functions are considered. It is found that a target function equal to the area of ripple of the magnetic field magnitude along the field line is very effective in reducing the neoclassical transport coefficient. © 1999 American Institute of Physics. [S1070-664X(99)01108-8]

## I. INTRODUCTION

Considered as fusion reactors, stellarators have several advantages over tokamaks. The main advantages are: stellarators are able to run in steady state operation, since they do not have to drive longitudinal electric current as tokamaks must do, and the very dangerous disruptive instability of tokamaks is absent in stellarators.

The main disadvantage of stellarators has been the high neoclassical transport loss rate. Due to the lack of axisymmetry in stellarators, particle orbits can have very large excursions from magnetic surfaces, thus increasing the transport coefficients in the reactor relevant, low-collisionality regime. However, the results of investigations during the last decade have shown that the violation of axisymmetry does not necessarily lead to deterioration of plasma particle confinement. It is found that good confinement of the particles is possible in three-dimensional, magnetohydrodynamic (3D MHD) configurations through the prudent choice of the plasma boundary shape.<sup>1,2</sup>

Also, present day and planned stellarators, both conventional ones and ones with improved plasma confinement, all have large aspect ratio and thus suffer economic difficulties due to low wall loading.

A new experiment, the proposed National Compact Stellarator eXperiment (NCSX)<sup>3</sup>, hopes to surmount these two deficiencies of stellarators by using the concept of quasi-axisymmetry to enhance plasma confinement and use boot-

strap current to decrease the aspect ratio, which will in turn increase the wall loading. It is hoped that in spite of the net plasma current it will be possible to have disruption-free discharges due to the existence of an external rotational transform.<sup>4</sup>

It is desired then to find a stellarator configuration with good confinement properties, good stability and good bootstrap current alignment. Since it is, in general, difficult to meet all these requirements, it is desirable to have as weak a constraint as possible on the properties giving good confinement. Most of the transport optimized configurations for NCSX have used the principle of quasisymmetry (QS) to reduce the transport. To obtain a QS configuration one must reduce the  $n \neq 0$  harmonics of the magnetic field strength  $B_{mn}$  in Boozer flux coordinates to zero. However, as was shown in Ref. 5, the exact fulfillment of the QS condition throughout the entire plasma column is impossible and thus one usually tries to minimize the  $n \neq 0$  harmonic. A more general approach to transport reduction and one that should be less constraining than QS in regards to the other optimization targets, such as stability, is pseudosymmetry (PS).<sup>6</sup> Results of optimization seeking PS configurations are discussed in the present paper.

The paper is organized as follows. In Sec. II, the formulation of the PS condition is presented and the difference between QS and PS conditions is analyzed. In Sec. III, the codes and tools used in the numerical calculations are dis-

cussed. In Sec. IV, possible target functions for pseudosymmetry optimization are discussed. In Sec. V, a comparison of several configurations is made, including ones optimized for QS, for PS, for a combination of PS and iota profile. The last section contains the conclusions.

## II. PSEUDOSYMMETRY

Fulfillment of the QS condition implies that the lines  $B = \text{const}$  on magnetic surfaces are straight in Boozer flux coordinates. (In addition, the field lines themselves are straight, as required for Boozer coordinates.) For charged particles, a QS system looks axisymmetric if:

- (1) there are no locally trapped or trapped-transition particles;
- (2) bounce averaged trajectories lie on a magnetic surface;
- (3) the radial width (in terms of flux coordinate) of the “banana” orbit of a trapped particle is constant as the particle drifts along the line  $B = \text{const}$ .

Particles are called “trapped-transition” if the maximum value of  $B$  as a function of  $\theta$  is not constant as the particles precess. These particles can be trapped for some  $\zeta$ , after which they could have a trajectory as transition particles.

If requirement (3) above is omitted, the configurations are called omnigenous systems. As was shown in Ref. 6, for QS systems the condition of omnigenicity can be fulfilled locally only, e.g., near the minimum of  $B$ , so that the system will be omnigenous for deeply trapped particles.<sup>7</sup> The requirement of omnigenicity on the whole magnetic surface<sup>8</sup> is equivalent to the QS condition.

If condition (1) is satisfied, the system is defined as pseudosymmetric. PS is the least restrictive of the enhanced transport schemes and can be satisfied, at least formally, in the entire plasma column.<sup>9</sup> Thus, in PS configurations, the lines  $B = \text{const}$  can be used as the coordinates lines  $\theta_{ps} = \text{const}$ . If it is possible to use  $\theta_{ps} = \text{const}$  as the poloidal coordinate, we can then deform the longitudinal coordinate in such a way that  $\theta_{ps}$ ,  $\zeta_{ps}$  are straight magnetic field line coordinates, and locally trapped and trapped-transition particles will be absent and the system will be pseudosymmetric.

In contrast to the QS condition, PS allows the lines  $B = \text{const}$  on the magnetic surface in Boozer coordinates to not be straight. However, if the slope of  $B = \text{const}$  lines relative to the  $\zeta_B$  axis exceeds the slope of the magnetic field lines for the configuration, locally trapped particles will exist and the system will not be PS. Thus, systems with large rotational transform per period allow the largest configurational difference between QS and PS systems.

## III. TOOLS: NUMERICAL CODES

### A. 3D Equilibrium Code

We use the fixed boundary version of the VMEC code<sup>10</sup> to obtain 3D MHD stellarator equilibrium with net toroidal current. Net toroidal current is an essential feature of NCSX.

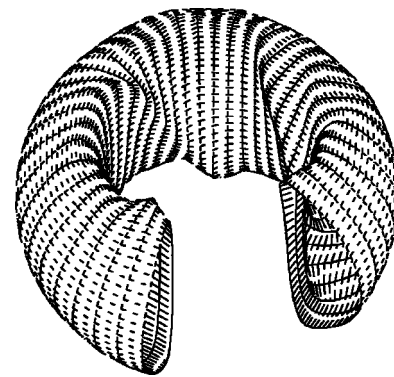


FIG. 1. 3D view of the boundary magnetic surface of the NCSX configuration, ksa14-11.

The VMEC input file describes the magnetic surface boundary in the form of a Fourier spectrum of the cylindrical coordinates  $R, \phi, Z$ ,

$$R(s, \theta, \zeta) = \sum R_{mn} \cos(m\theta - n\zeta),$$

$$Z(s, \theta, \zeta) = \sum Z_{mn} \sin(m\theta - n\zeta),$$

$$\phi = \zeta/N.$$

Here  $s$  is the radial flux coordinate proportional to the normalized toroidal flux, with  $s=1$  on the boundary magnetic surface,  $\zeta$  is a toroidal angle increasing by  $2\pi$  for one system period,  $\theta$  is a poloidal angle, and  $N$  is the number of stellarator periods.

To illustrate our results, we consider a four-period case of NCSX, designated as ksa14-11 (Fig. 1). It has a major radius  $R_{00} = 4.96m$ ; the minor plasma radius is determined by the components  $R_{10} = 1.74m$  and  $Z_{10} = 3.24m$ . The plasma cross section of this configuration has a relatively high elongation and low aspect ratio. This configuration can be scaled to fit into the PBX tokamak chamber with a major radius  $R = 1.5m$ . ksa14-11 was one of the candidate configurations for the NCSX experiment.

The ksa14-11 configuration is obtained from helically perturbing an ARIES<sup>11</sup> tokamak configuration while maintaining quasi-axisymmetry. ksa14-11 uses the current profile of ARIES, which has 90% of its rotational transform,  $\iota$ , from the bootstrap current at a beta of 7.5%. The current and pressure profiles are fixed during our optimization run.

The VMEC input boundary Fourier components  $R_{mn}, Z_{mn}$  have poloidal mode number  $m_{\text{max}} = 5$ , toroidal number  $n_{\text{max}} = 3$ , and the total number of boundary modes,  $R_{mn}, Z_{mn}$  equal to 23. We use 48 radial plasma grid points.

### B. MAPPING CODE

The 3D numerical calculations of neoclassical transport need a representation of the magnetic field in Boozer coordinates  $s, \theta_B, \zeta_B$ . The magnetic field in the VMEC output file is represented in a nonstraight flux coordinate system. The transformation from VMEC to the Boozer coordinate system

is performed by a part of the JMC code<sup>12</sup> extracted by H. Gardner. A Fourier spectrum of the magnitude of the magnetic field consists of 304 modes,

$$B(s, \theta_B, \zeta_B) = \sum_{m,n} B_{mn}(s) \cos(m\theta_B - n\zeta_B),$$

where the maximum poloidal number  $m$  is 15, and the maximum toroidal number  $n$  is 9. We performed these calculations with a larger number of modes in Boozer coordinates to ensure that the equilibria are accurately represented in the nonoptimal Boozer coordinates.

### C. Monte-Carlo code

The Monte-Carlo calculation of the diffusion coefficient is done with the GC3 code<sup>13</sup>. GC3 is a guiding-center code in Boozer coordinates, and uses only the largest of the  $B_{mn}$  harmonics (typically  $m=10$  and  $n=16$  modes). In these simulations the monoenergetic ensembles are simulated with 352 particles, with a kinetic energy of  $K=2T$ , evenly distributed in pitch  $v_{\parallel}/v$ ,  $\theta_B$ , and  $\zeta_B$ . A Lorentz collision operator is used. The rotational transform profile of  $\iota$  is determined from the fit  $q(s) = q_{ax} + s(q_{mx} - q_{ax})$ , where the safety factor  $q = 1/\iota$ ,  $q_{ax}$  and  $q_{mx}$  correspond to the values of  $q$  at the axis ( $s=0$ ) and at the edge ( $s=1$ ). In our calculations we use a density profile which is parabolic-squared in the averaged minor radius.

GC3 has not yet been optimized for speed, so the ensemble size used is modest. However, it has recently been benchmarked against the ORNL code of Rome, Fowler and Lyon,<sup>14</sup> which yields results, using much larger ensembles, within 15% of GC3.

One run of GC3 takes about an hour on the C90 computer, too long to be included in a transport optimization loop. Therefore, for transport optimization, we use a target function which is functional of  $B$ . The evaluation of this target function is much faster than using GC3. After optimizing a configuration for transport using the target function, we use the GC3 code to check the value of the diffusion coefficient to insure we have found an optimized configuration.

## IV. TARGET FUNCTIONS

In searching for configurations with enhanced plasma confinement we must vary a large number of parameters, which are the harmonics specifying the boundary shape. Typically, there are about 23 of these parameters. To find the optimal value of the boundary harmonics for minimizing transport, a target function is selected and an optimizer is employed. We now discuss three choices of the target function,  $X$ , HILL and WATER for PS configurations.

### A. X function

In the first article to discuss quasihelical symmetry,<sup>1</sup> the target function of the optimization was the ratio,  $X$ , symmetric component,  $B_{1,1}$ , at the plasma edge to the major Fourier component of  $B$  that violates the helical symmetry. Approximately one order of magnitude (i.e.,  $X=10$ ) was achieved. This leads to a significant reduction of neoclassical transport in the Helias configuration.<sup>15</sup>

The same result was obtained for HSX (Helically Symmetric eXperiment at Wisconsin),<sup>16</sup> where the ratio  $X$  is about 15, and the diffusion coefficient is similar to that of tokamaks.

However, the target function,  $X$ , is not always effective for QS optimization. We find that increasing  $X$  can lead to an expansion of the Fourier spectrum of  $B$ , with the consequences that the large number of small nonsymmetric harmonics of  $B$  can add together to degrade confinement. Such a case is discussed in the next section.

### B. Hill function

As was mentioned above, the condition of pseudosymmetry is more general than QS. The PS condition permits the Fourier spectrum in Boozer coordinates to have nonsymmetric harmonics, and thus a target function like  $X$  above is too restrictive to access all the PS configurations.

One characteristic feature of PS systems is the absence of islands of lines  $B=\text{const}$  on magnetic surfaces. Thus, the elimination of such islands is a necessary condition of pseudosymmetry. We call the target function which we will use to eliminate islands, HILL.

As a first step in defining the target function HILL, one finds the coordinates of the  $x$ - and  $o$ -points of the function,  $B(\theta_B, \zeta_B)$ , in one system period. Next one finds closed contours of  $B=\text{const}$  and calculates the heights  $H_i$  of the  $o$ -points relative to their  $x$ -points. Explicitly,  $H_i = |(B_{o_i} - B_{x_i})|$ , where  $(B_{o_i})$  is  $B$  at the  $o$ -point labeled  $i$  and  $(B_{x_i})$  is  $B$  at the corresponding  $x$ -point labeled  $i$ . Techniques like this are used in geography and in the other sciences where one needs to describe the properties of mountainous surfaces. Once the above operations are performed, the target function HILL,  $H$ , can be defined as the  $\max(H_i)$ .

One problem with the HILL target function is that  $H$  has a strong dependence on a small modulation of  $B(\theta_B, \zeta_B)$  function. Small modulations can form additional  $x$ - and  $o$ -points that can increase the target function significantly.

In addition, the condition of the absence of islands in the  $B$  contours is necessary but not sufficient for pseudosymmetry: if the magnetic field line is tangent at some point to the line  $B=\text{const}$ , locally trapped particles can still exist in the configuration.

### C. Water function

The fulfillment of the PS condition means that there are no local minima or maxima, except for the maximum (inboard) and minimum (outboard) that occur because of the  $1/R$  variation of the main toroidal field, on the curve  $B(l)$ , where  $l$  is the distance along a line of force. This condition implies the absence of the locally trapped particles. In an attempt to fulfill this condition, we have used the target function we call WATER.

The WATER function calculates the total area of the ripple  $W$  for half of one poloidal turn of the force line. To calculate  $W$  one needs to sum the amount of "water" trapped in all local wells. Figure 2 illustrates a local ripple filled by "water." The target function,  $W$ , can be computed

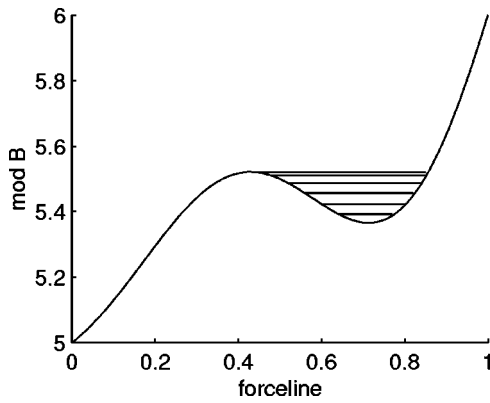


FIG. 2. An example of one local ripple of  $B$  filled by the “water.”

very rapidly using any number of  $B_{mn}$  modes. It should be noted that the condition  $W=0$  does not coincide exactly with the condition of absence of locally trapped particles since the curve  $B(l)$  is not a periodic function. However, since the rotational transform per period is small for the cases considered here,  $W=0$  should be a good prescription for minimizing the number of locally trapped particles.

**V. OPTIMIZATION RESULTS**

**A. The test configuration—ksa14-11**

The configuration used to test our optimization procedures is a configuration mentioned above, ksa14-11. The Fourier spectrum of the magnetic field strength has relatively large components  $B_{1,-1}$ ,  $B_{2,-1}$ ,  $B_{1,2}$ ,  $B_{2,-2}$  (see Fig. 3) destroying the quasi-axisymmetry. The ratio  $X=B_{1,0}/B_{1,-1}=5.78$  for a surface in the middle of the plasma ( $s=0.5$ ) is low. As a result, there are large ripples of  $B$  along the force line and closed contours of  $B$  (see Fig. 4) are formed around three large hills. The highest hill of  $B$  has a height  $H=(B_o - B_x)/B_o=0.082$ , again for a radius in the middle of the plasma.

**B. HILL optimization—max2 configuration**

Our first attempt to optimize ksa14-11 used the HILL target function,  $H$ . As a result of this optimization the height of the highest hill was reduced to  $H=0.045$ . This result was

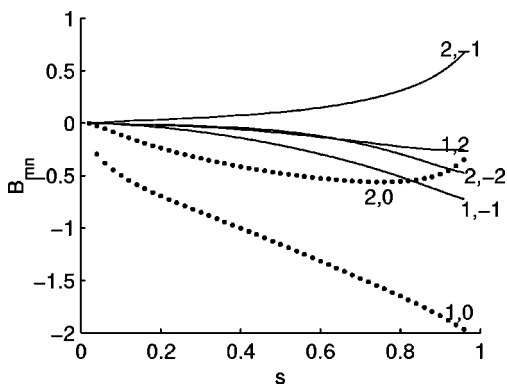


FIG. 3. The largest Boozer components  $B_{mn}$  of the magnetic field strength as a function of plasma flux surface  $s$  for the configuration ksa14-11.

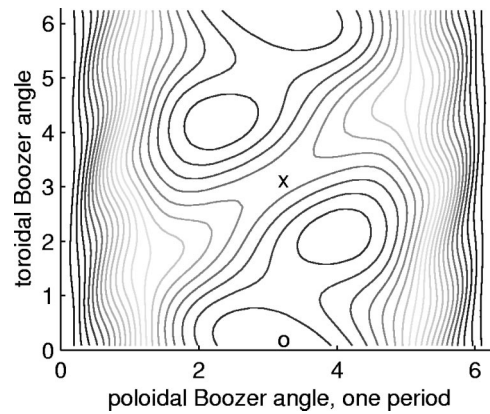


FIG. 4.  $B$ -contours on the middle plasma flux surface  $s=0.5$  for the case ksa14-11; the height of the highest hill is  $H=(B_o - B_x)/B_o=0.082$ , where  $B_o$  is a point of the maximum of  $B(\theta_B, \zeta_B)$  function, and  $B_x$  is a corresponding  $x$ -point value of  $B$  function.

obtained mainly by increasing the value  $B_x$  at the  $x$ -point of the function  $B$ . We label this configuration max2 and plot it in Fig. 5. The new  $B$  function has three hills of almost the same height. There was very little reduction in the size of the local wells. Efforts to minimize the height of the hills typically leads to growth of more hills and local wells. Another problem with the HILL target function is the difficulty of keeping track of the changing topology of the hills and valleys. The topology typically changes very rapidly as we vary the plasma boundary.

**C. X optimization—max3 configuration**

Our next attempt at optimizing the ksa14-11 configuration used the  $X$  target function which was described above. The mode most responsible for destroying the quasi-axisymmetry of ksa14-11 is the  $B_{2,-2}$  mode. We were able to increase the value of  $X$  from 5.8 for the ksa14-11 configuration (Fig. 3) to 20 for the configuration we call max3. However, as we found for the HILL target function and shown in Fig. 6, we were unable to significantly reduce the large ripple wells. This can be explained by the fact that

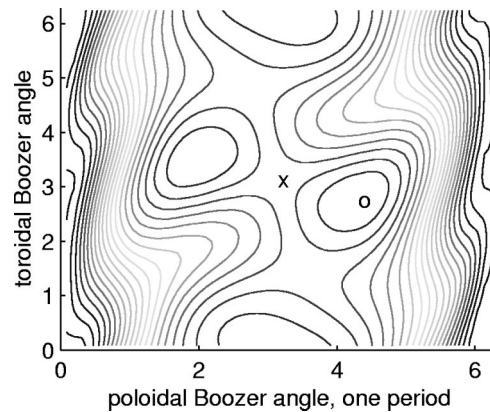


FIG. 5.  $B$ -contours on the middle plasma flux surface  $s=0.5$  for configuration max2. The height of the highest hill is  $H=0.045$ .

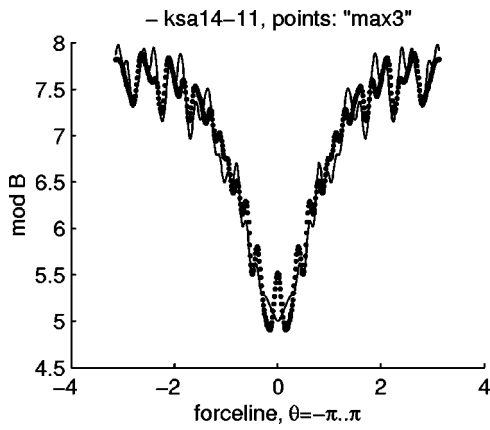


FIG. 6. The magnetic field strength  $B$  on the middle plasma flux surface  $s = 0.5$  versus the field line on one poloidal turn for the cases max2 and max3. A significant ripple can be seen even for a large ratio  $X$  (max3 case).

small nonsymmetric  $B_{mn}$  modes can give a large sum at some points along the field line, resulting in large ripples of  $B$  along the field line.

**D. WATER optimization—max5 configuration**

Since the max3 configuration showed that maximizing the  $X$  target function can lead to an increase of the ripple amplitude and hence to an increase of neoclassical losses, we next tried to minimize the ripple directly by using the WATER target function. For the resulting configuration, max5, we were able to lower  $W$  by a factor of ten over that of initial configuration, ksa14-11. The max5 configuration is very nearly completely pseudosymmetric. There is only one closed  $B$ -contour near  $B_{max}$  for a flux surface in the middle of the plasma column. The Boozer spectrum of the pseudosymmetric case, max5, differs significantly from the quasi-axisymmetric case, max3, (see Fig. 7). The ratio  $X$  for the max5 case is 15.5, and is less than the value of  $X = 20$  for the quasi-axisymmetric case, max3. These results show that a large ripple does not necessarily imply a small value of  $X$  and that a large value of  $X$  does not imply low ripple.

The neoclassical diffusion coefficient of this pseudosymmetric configuration, max5, was checked using the GC3 code.

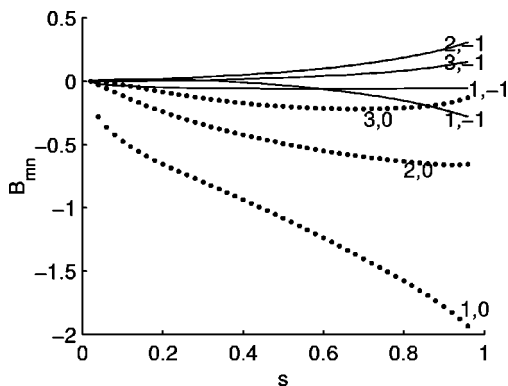


FIG. 7. The largest Boozer components  $B_{mn}$  of the magnetic field strength as a function of plasma flux surface  $s$  for configuration, max5. The ratio  $X$  at  $s = 0.5$  is 15.

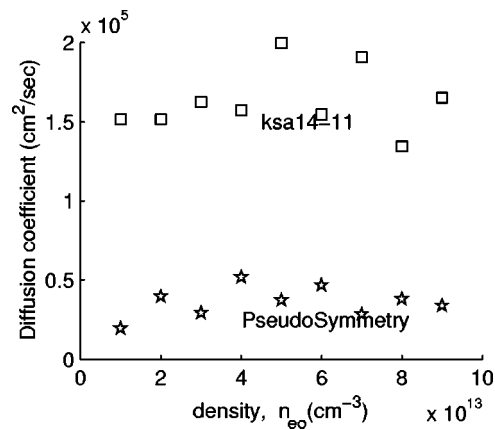


FIG. 8. The diffusion coefficient  $D$  versus plasma density  $n_{e0}$  for pseudosymmetric case, max5, and the initial case ksa14-11.

We made GC3 runs using 16 of the largest  $B_{mn}$  and compare the corresponding calculation for the initial case ksa14-11. The diffusion coefficients as a function of particle density for the max5 and ksa14-11 configurations are presented in Fig. 8. The diffusion coefficient of the pseudosymmetric case, max5, is roughly five times smaller than ksa14-11.

**E. WATER and iota optimization—max6 configuration**

The max5 configuration demonstrated that pseudosymmetry is achievable and that the resulting configuration has good transport properties. However, the iota profile changed during the optimization of max5 and a question arises as to whether pseudosymmetry can be achieved with the added constraint that the iota is fixed. This is an important question since the iota profile was arrived at by optimizing the configuration for stability and we would like to have the final configuration have nearly the same stability properties as the original configuration. Hence we targeted four functions in the optimizer: the iota values at the axis and at the edge, the value of  $\beta$  and the value of WATER target function.

We call the resulting configuration, max6. The iota profiles for the reference case ksa14-11 and for the cases max5

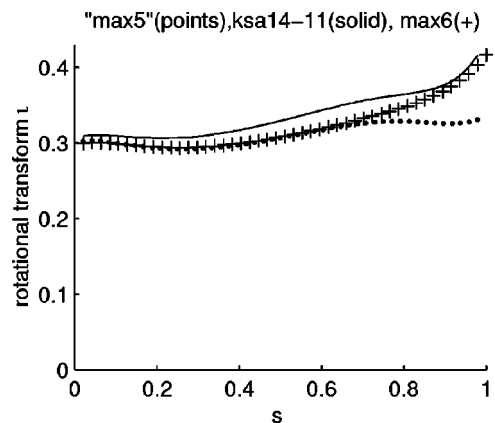


FIG. 9. The rotational transform  $\iota$  as a function of plasma flux surface  $s$  for the initial case ksa14-11 and for the cases max5 and max6. It can be seen that the iota values at the edge and at the axis of max6 case are very close to the values of the reference profile of ksa14-11 configuration.

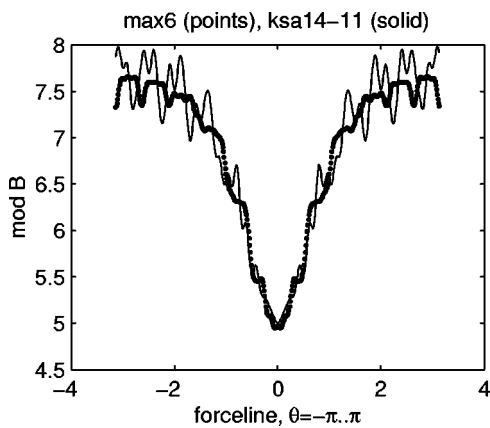


FIG. 10. The magnetic field strength  $B$  on the middle plasma flux surface  $s=0.5$  versus the field line on one poloidal turn for the pseudosymmetric max6 and ksa14-11 configurations. The ripple area  $W$  for the max5 case is seven times less than for the initial ksa14-11 case.

and max6 are shown in Fig. 9. It can be seen that the iota values at the edge and at the axis of max6 case are very close to the values of the reference profile of the ksa14-11 configuration. This is not so for configuration max5.

The magnetic field strength  $B$  on the middle plasma flux surface along the field line for one poloidal turn for the max6 configuration is shown in Fig. 10. The ripple area,  $W$ , for max6 case is seven times less than the reference case ksa14-11 and is a little bit larger than that for the max5 configuration.

The neoclassical diffusion coefficient of the max6 configuration was calculated with the GC3 code using ten of the largest  $B_{mn}$  components and compared the corresponding calculation for the initial case ksa14-11. The diffusion coefficients as a function of particle density for max6 and ksa14-11 configurations are presented in Fig. 11. The diffusion coefficient of the pseudosymmetric configuration max6 is roughly five times smaller than the ksa14-11 case, and is

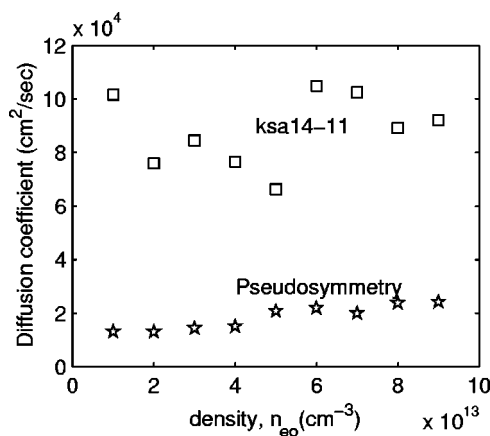


FIG. 11. The diffusion coefficient  $D$  versus plasma density  $n_{e0}$  for pseudosymmetric case, max6, and the initial case ksa14-11 using ten main Boozer  $B_{mn}$  modes as GC3 code input.

very close to the diffusion coefficient of the max5 configuration. Thus, optimized configurations with pseudosymmetry, low neoclassical transport, and targeted values of  $\beta$  and iota profile have been shown to exist.

### F. Summary

The purpose of this research was to apply the concept of pseudosymmetry to improve the neoclassical transport properties of an NCSX four-period configuration. Pseudosymmetry is a more general and less restrictive method for obtaining good neoclassical confinement than quasi-axisymmetry. To obtain pseudosymmetry configurations, several target functions were used: X, HILL and WATER. Of the three, WATER was the most successful. Using the WATER target function we obtained a configuration with ten times less ripple area and five times smaller diffusion coefficient than the reference configuration. We were also able to obtain a configuration that had small ripple area, and the same  $\iota$  profile as the reference configuration.

Our future plans are to use our target function  $W$  in conjunction with a stability code built into the optimizer, so that we can achieve both low neoclassical transport and a high value of  $\beta$  with respect to stability.

### ACKNOWLEDGMENTS

We thank Dr. S. P. Hirshman for use of the VMEC equilibrium and optimizer codes, and Dr. H. Gardner for use of the Mapper code. This work was sponsored by the U.S. Department of Energy, Contract No. DE-AC02-76CH03073.

- <sup>1</sup>J. Nuehrenberg and R. Zille, Phys. Lett. A **129**, 113 (1988).
- <sup>2</sup>P. Garabedian, Phys. Plasmas **3**, 2483 (1996).
- <sup>3</sup>D. A. Monticello, G. Y. Fu, R. Goldston *et al.*, "Physics Consideration for the Design of NCSX," *Proceedings 25th EPS Conference on Controlled Fusion and Plasma Physics Prague, 1998* (European Physical Society, Petit-Lancy), paper 1.187 (to be published).
- <sup>4</sup>WV7-A Team, Nucl. Fusion **20**, 1093 (1980).
- <sup>5</sup>D. A. Garren and A. H. Boozer, Phys. Fluids B **3**, 2822 (1991).
- <sup>6</sup>V. D. Shafranov, M. I. Mikhailov, A. A. Skovoroda, and A. A. Subbotin, *Proceedings of International Symposium on Plasma Dynamics in Complex Electromagnetic Fields - for Comprehension of Physics in Advanced Toroidal Plasma Confinement, 8-11 December, 1997*, Research Report, Inst. of Advanced Energy, Kyoto University, March 20, 1998, p. 193 (Kyoto University, Gokasho, Uji 611, Japan, 1998).
- <sup>7</sup>S. Gori, W. Lotz, and J. Nuehrenberg, *Joint Varenna-Lausanne Int. Workshop on Theory of Fusion Plasmas*, edited by J. W. Connor, E. Sindoni, and J. Vaclavik (Societa Italiana di Fisica-Editrice Compositori, Bologna 1996), p. 335.
- <sup>8</sup>J. R. Cary and S. G. Shasharina, Phys. Rev. Lett. **78**, 674 (1997).
- <sup>9</sup>M. I. Mikhailov, V. D. Shafranov, and D. Sunder, Plasma Phys. Rep. **24**, 653 (1998).
- <sup>10</sup>S. P. Hirshman and O. Betancourt, J. Comput. Phys. **96**, 99 (1991).
- <sup>11</sup>S. C. Jardin, C. E. Kessel, C. G. Bathke *et al.*, Fusion Eng. Des. **38**, 27 (1997).
- <sup>12</sup>J. Nuehrenberg and R. Zille, *Proceedings 5th International Workshop on Stellarators*, Schloss Rinberg, 1984 (Commission of the European Communities, Brussels, 1984) EUR 9618EN 339.
- <sup>13</sup>H. E. Mynick, Plasma Phys. Rep. **23**, 547 (1997).
- <sup>14</sup>R. H. Fowler, J. A. Rome, and J. F. Lyon, Phys. Fluids **28**, 338 (1985).
- <sup>15</sup>W. Lotz, 2nd Ringberg Workshop on W-7X, 1988 (Commission of the European Communities, Brussels, Belgium, 1988), p. 97.
- <sup>16</sup>F. S. B. Anderson, A. Almagri, D. T. Anderson, P. G. Matthews, J. N. Talmadge, and J. L. Shohet, Trans. Fusion Tech. **27**, 273 (1995).